Effect of strain path change on precipitation behaviour of Al-Cu-Mg-Si alloy

S Mishra[1], K Kulkarni[2], N P Gurao[2]

[1]Department of Materials Science and Engineering, Indian Institute of Technology Kanpur, Kanpur-208016, India

[2]Department of Materials Science and Engineering, Indian Institute of Technology Kanpur, Kanpur-208016, India

E-mail: npgurao@iitk.ac.in

Abstract. The effect of strain path change on precipitation behaviour of Al-Cu-Mg-Si alloy was investigated. Two different types of crystallographic textures were produced by changing the strain path during rolling. The deformed samples were subjected to a short recrystallization treatment and ageing to identify the effect of strain path change manifested in terms of crystallographic texture on precipitation behaviour. Preliminary characterization indicates that ageing kinetics as well as precipitate morphology vary depending upon the mode of rolling. The coherency strains associated with a coherent interface is relieved in a unlike manner for differently rolled samples.

1. Introduction

Precipitation hardening is produced by solutionizing and quenching an alloy in which the second phase precipitates out upon ageing at intermediate temperature. The requirement of a precipitation-hardening alloy is that the phase diagram should show a solvus viz. solid solubility limit should decrease with decrease in temperature. The driving force behind rejection of excess solutes in the form of the precipitates is supersaturation [1, 2]. The sluggish diffusion kinetics at low temperatures ensures that the solute atoms move through only a few tens of interatomic distance [3, 4], hence giving rise to precipitation on a very fine scale. The precipitates of the second phase are generally coherent in nature. If the mismatch between the lattice of matrix and precipitate is large, then considerable amount of coherency strain is associated with a coherent interface, giving rise to internal strain hardening. The main contribution to hardening comes from the interaction between the moving dislocations with finely dispersed precipitates [5, 6]. The Al 6XXX alloys are precipitation hardenable alloys and precipitation hardening is the key aspect behind high strength to weight ratio of these alloys. The decomposition of supersaturated solid solution occurs is several steps involving transition precipitates before the equilibrium precipitate forms [7, 8]. Generally the nucleation barrier for the formation of equilibrium precipitate is too high. The prerequisite of surface energy to create surfaces of critical-sized precipitates dominates over volume Gibbs free energy decrease during the initial stages of precipitation. Usually a sheet of age-hardenable material undergoes some sought of thermo-mechanical processing involving deformation at room temperature and ageing at slightly elevated temperature [9, 10]. Since the recrystallization temperature is higher than the ageing temperature, the alloy retains the polygonised structure, which has high density of dislocations. Thus, precipitation is more fine and homogeneous due to their precipitation on dislocation substructure. Thus, a proper amalgamation between various deformation techniques and ageing cycle is needed to develop attractive mechanical properties. In addition to introduction of dislocations and other lattice defects during deformation, there is also evolution of strong texture in the material. Thus proper scrutiny of texture is required to develop such beneficial properties. Previous investigations indicate that by changing the strain path during room temperature plastic deformation, characteristically different texture can be obtained in the same material [11, 12]. Essentially the deformation substructure is destabilized. Physical phenomena's like

recrystallization and phase transformation are also affected by a change in strain path during plastic deformation [13, 14]. Thus, it is worth paying attention on the effect of different deformation texture on precipitation behaviour in age-hardenable alloys. The key is to separate out the effect of crystallographic texture from other microstructural parameters like grain size, dislocation density, micro-strain etc. Thus, the intention behind the present investigation is to examine the effect of different initial textures obtained via strain path change on precipitation behaviour in Al-Cu-Mg-Si alloy.

2. Experimental

2.1. Thermo-mechanical-processing

Hot rolled plates of Al-Mg-Si-Cu alloy in T6 temper was used as starting material for present investigation. To wipe out the previous plastic deformation history the hot rolled plate was subjected to solutionizing treatment in a muffle furnace for 24 hrs, followed by quenching in water. The solutionized plates were rolled in multiple passes at room temperature in two different ways with the true strain being constant for each pass. In uni-directional rolling (UDR) the samples are rolled down to final thickness viz. 1 mm without changing the strain path or the rolling direction. In multi-step cross rolling (MSCR) the sample is rotated by 90^{o} after each pass [11, 12]. A brisk recrystallization technique consisting of holding the rolled samples at 500^{o}C for two minutes in a salt bath furnace, followed by quenching in water was devised to detach the effect of crystallographic texture from other microstructural parameters. The recrystallized samples were subjected to ageing at 160^{o}C in an oven to appreciate the effect of texture on precipitation behaviour in an age-hardenable alloy.

2.2. Characterization

The pole figures were measured at half thickness of the RD-TD plane using Bruker D-8 Discover texture goniometer. For bulk texture determination of the matrix (111), (200), (220) and (311) pole figures were measured assuming triclinic sample symmetry. Zeisss EVO 50 scanning electron microscope (SEM) attached with an electron back scatter diffraction (EBSD) unit from Oxford Instruments was used to carry out the microstructural investigation. It was ensured that step size and binning were kept at 0.5 μm and 4*4 respectively. The electron transparent region required for Transmission electron microscopy (TEM) was produced using PIPS (precision ion milling system). The samples were analysed in a Tecnai-G2-Ultra Twin TEM.

3. Results and discussion

3.1. Texture

The (111) pole figures for the UDR and MSCR samples, after recrystallization at 500^{o}C for 2 minutes (here after referred as UDRX and MSCRX) and for UDRX and MSCRX samples aged at 160^{o}C upto peak ageing condition (UDRXA and MSCRXA) are shown in Fig.1. The bulk texture measurements clearly underline the fact that texture is noticeably different for differently processed samples, while there is no distinctive difference in texture upon peak ageing. The texture of UDRX sample is outlined by the presence of {100} <001> cube component along with a substantial amount of {100} <110> and {110} <112> Brass component. On the other hand the texture for MSCRX samples is appreciably different from the UDRX samples. The MSCRX samples show a dominant cube component with few traces of Brass component. The important point is that there is absence of {100} <110> component in MSCRX samples. From the pole figures it can be deduced that there is no characteristic change in texture during ageing of recrystallized samples, apart from strengthening and weakening of few components. The UDRXA sample shows an augment in Brass component while the cube component decreases. The key difference is that cube component is still the dominant component in MSCRXA with hardly any traces of Brass component. Thus, change in strain path during rolling causes an appreciable difference in texture for UDRX and

MSCRX samples. The texture is relatively weaker for MSCRX samples [11, 12]. This can be attributed to the fact that there is continual destabilization of deformation substructure along with a change in the frame of reference for MSCRX samples [11, 12]. The characteristic deformation texture evolved during rolling leads to a distinct recrystallization texture on annealing for the differently rolled samples.

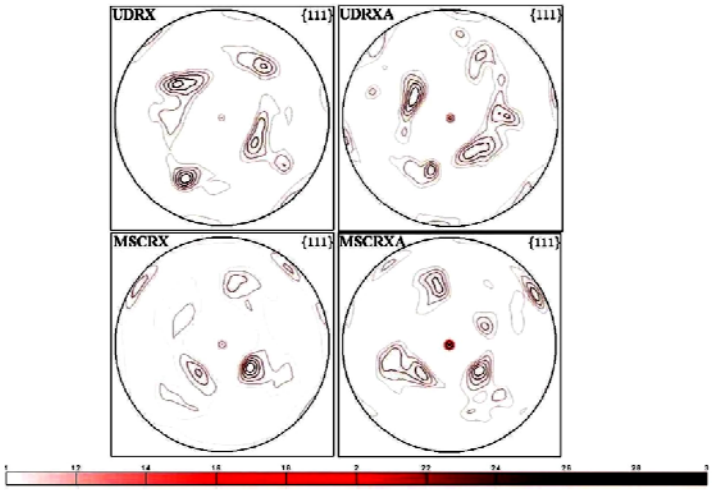

Fig. 1 (111) pole figures of UDRX, UDRXA, MSCRX and MSCRXA.

3.2. Microstructure

Figure.2 represents the EBSD analysis of UDRX, UDRXA, MSCRX and MSCRXA samples. As evident from Figure.2, the microstructure consists of well recrystallized grains with minimal variation in grain size for UDRX (~9 ± 7 μm) and UDRXA (~ 9.5 ± 8μm) samples. A similar trend is observed for MSCRX (~8 ± 7μm) and MSCRXA (~ 12 ± 10μm) samples. Also there is a minimal difference in grain size for UDRX and MSCRX samples. Thus, grain sizes are comparable and no appreciable amount of grain growth has taken place during ageing.

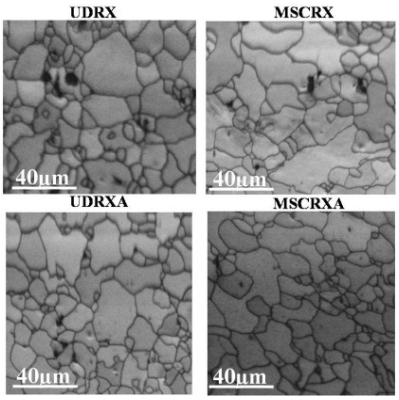

Fig. 2 EBSD micrographs of UDRX, UDRXA, MSCRX and MSCRXA.

The local average misorientation map (LAM) for UDRX, UDRXA, MSCRX and MSCRXA is given in Figure.3. This component calculates small orientation changes on the map, thus highlighting regions of higher deformation. It calculates the misorientation between every pixel and its neighbouring pixel and assigns an average value to that pixel. Figure.3 clearly brings out the fact that recrystallization is more or less complete for UDRX and MSCRX. The lower values of local misorientation angle within the grains suggest that complete recrystallization has taken place with few remaining traces of deformed regions. As expected, the average local misorientation angle is on the higher side near the grain boundaries. During

ageing of the recrystallized samples coherent and semi-coherent metastable precipitates form within the matrix. This produces elastic lattice strains called 'coherency strains' across the boundary where the lattice planes must be bent to achieve this one to one matching. Coherent precipitates have low interfacial energy, but they are associated with coherency strains. A semi-coherent precipitate will have high interfacial energy but the coherency strains will be relieved. If the misfit between the matrix and the precipitate is on the higher side then it becomes energetically favourable to relieve the coherency strains by introducing geometrically necessary dislocations or misfit dislocations within the matrix. Thus, a semi-coherent boundary consists alternately of region of coherency and region of disregistry. As evident from Figure.3 the average local misorientation angle is on the higher for MSCRXA compared to UDRXA. This suggests sluggish ageing kinetics for MSCRXA. The β' precipitates are taking more time to lose their coherent character and thus the magnitude of coherency strains is on the higher side for MSCRXA compared to UDRXA. Thus, more number of misfit dislocations are introduced in to the matrix for MSCRXA. This causes the average local misorientation angle to be on the higher side for MSCRXA.

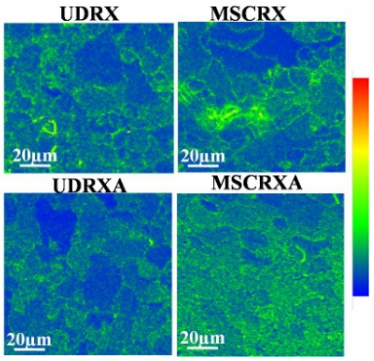

Fig. 3 Local average misorientation angle map (LAM) of UDRX, UDRXA, MSCRX and MSCRXA.

3.3. TEM-studies

The TEM bright field micrograph for UDRXA and MSCRXA samples are shown in Fig.4. The presence of intragranular β' precipitate within the matrix of aluminium aged upto peak ageing condition is evident from the representative TEM micrographs. The vital point is that the aspect ratios of precipitates are different for both the cases. The aspect ratio is on the higher side for UDRXA samples i.e. (~3:1) compared to MSCRXA (~1.2:1). This morphological anisotropy can be attributed to difference in ageing kinetics for UDRX and MSCRX. The faster ageing kinetics for UDRX suggests that precipitates are losing their coherent character earlier than MSCRX. For plate shaped precipitates it is possible to nucleate dislocations at the interface by developing stresses higher than the theoretical strength of the matrix at the edges of the plate [15]. As the plate grows the same process is repeated in order to maintain constant spacing between the dislocations. It has already been shown that plate like precipitates lose their coherency by forming a dislocation loop within the precipitate [16]. The quenched-in mono-vacancies and di-vacancies get attracted towards the coherent interface and then condense to form a dislocation loop within the precipitate. The dislocation loop can expand within the precipitate and cause a simultaneous loss in coherent character. The effect of strain path is manifested in terms of different interface characteristics for UDRXA and MSCRXA, hence different precipitate morphology.

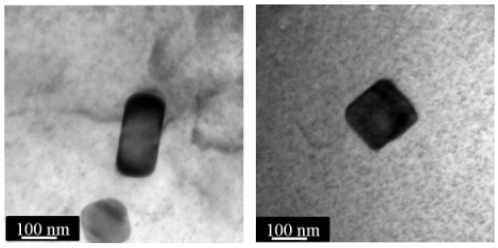

Fig. 4 TEM micrograph of UDRXA and MSCRXA.

Further investigations are needed for better understanding of the governing mechanism but it is quite clear that changing the strain path during rolling plays a key role in controlling the morphology of the precipitates and in the hindsight might also control the precipitation kinetics.

Conclusions

The present investigation clearly shows the effect of strain path change on precipitation behaviour of Al-Cu-Mg-Si alloy. In summary Al-Cu-Mg-Si alloys with different initial texture shows different precipitate morphology and varying texture can give a handle on developing isotropic and anisotropic properties in Al sheets. Crystallographic texture plays a key role in controlling the interface characteristics. The sluggish ageing kinetics for MSCRXA is manifested in terms of higher value of average misorientation angle. The coherency strains are relieved at a much smaller pace for MSCRXA compared to UDRXA. Thus, the growth of the precipitates is almost isotropic for MSCRXA compared to UDRXA where the coherent character of the interface is lost at a much higher pace, thus, leading to anisotropic growth.

References

[1] Smallman RE, Ngan AHW 2014, *Modern Physical Metallurgy* (Elsevier) 8th Edition, p 499
[2] Tilak RV, Morris JG 1985, *Mater. Sci. Eng.* **73**, 139
[3] Soffa WA, Laughlin D E 2014, *Physical Metallurgy* (Elsevier) 5th Edition, p 851
[4] Nie JF 2014, *Physical Metallurgy of Light Alloys* (Elsevier) 5th Edition, p 2009
[5] Ashby M 1966, *Acta Metall.*, **14**, 679
[6] Yang W, Ji S, Huang L, Sheng X, Li Z, Wang M 2014, *Mater. Charact.*, **94**, 170
[7] Son SK, Matsumura S, Fukui K, Takeda M 2011, *J. Alloy Compd.*, **509**, 241
[8] Fukui K, Takeda M, Endo T 2005, *Mater. Lett.*, **59**, 1444
[9] Sun DL, Yang DZ, Hong Y, Lei TC 1989, Proceedings of *ICSMA 8*, **2**, 591
[10] Ghosh SK 2011, *J. Mater. Sci. Technol.*, **27**, 193
[11] Suwas S, Singh AK 2003, *Mater. Sci. Engg. A*, **356**, 368
[12] Suwas S, Gurao NP 2014, *Comprehensive Materials Processing*, (Elsevier) vol. 3, p 81
[13] Garg R, Gurao NP, Ranganathan S, Suwas S 2011, *Philos. Mag.*, **91**, 4089
[14] Gurao NP, Ali A, Suwas S 2009, *Mater. Sci. Eng. A*, **504**, 24
[15] Porter DA, Easterling KE 1992, *Phase Transformation in Metals and Alloys*, (CRC Press London) 3rd Edition, p 160
[16] Sankaran R, Laird C 1974, *Philos. Mag.*, **29**, 179